Supplemental Data

Supplemental Figure Legends:

Supplemental Figure S1. Characterization of Alemtuzumab pharmacodynamics *in vivo* and possible effector mechanisms (related to Figure 1). (A) *In vivo* imaging of healthy NSG and leukemic hMB mice using a fluorescently labeled Alemtuzumab-AlexaFluor750 antibody. Mice were injected *i.v.* and euthanized 4h post injection. Skin was removed for total body imaging. **(B)** Quantitation of emitted light from defined regions covering the spleen and spine (as a representative of the bone marrow), comparing healthy NSG controls and leukemic hMB mice 4h post injection of alemtuzumab-AlexaFluor750 conjugate. **(C)** Direct assessment of spleen and bone marrow derived cells for *in vivo* bound Alemtuzumab-AlexaFluor750. **(D)** Assessment of complement–dependent cytotoxicity, using 20% sera *in vitro* vs. serum-free control. Dose-response to increasing alemtuzumab doses is shown by PI-stain and flow cytometry after 48h. **(E)** A macrophage-mediated ADCC assay comparing NSG and C57/BL6 derived macrophages with p47 phox $^{-/-}$ derived macrophages lacking the ability to produce reactive oxygen species (ROS) (Jackson et al., 1995). See also Supplemental Movie S1.

Supplemental Figure S2. Characterization of shRNA-mediated knockdown in hMB cell lines (related to Figure 2). (A) Western blot analysis of PTGES3 expression in mCHERRY^{+}-sorted control vector infected vs. shPTGES3 infected cells. Tubulin serves

as loading control. **(B)** Flow cytometry of FCGR2B expression in control cells vs. an shFCGR2B-infected cell line. **(C)** Flow cytometry of CD52 expression in control cells vs. a shCD52 infected mCHERRY^{+}-sorted cell line. See also Supplemental Table S1.

Supplemental Figure S3. Characterization of combinatorial effects of chemoimmunotherapy (related to Figure 3) (A) Evaluation of the minimal cyclophosphamide required dose for synergy with alemtuzumab. Cyclophosphamide co-treatment was systematically reduced using 1 day and 2-day regimens. Minimal required dose for the maintenance of synergy was 100 mg/kg or 2 x 50 mg/kg (n=5, SEM). **(B)** Follow-up analysis of leukemic burden in peripheral blood of treated vs. untreated mice. Flow cytometry of 20 µl peripheral was performed. **(C)** Combinatorial approaches using conventional frontline chemotherapeutics cytarabine (ARA-C; 1X 100 mg/kg), bendamustine (BENDA, 2x 25 mg/kg) and chlorambucil (2x 5 mg/kg) in combination with alemtuzumab (Alem., 2x 5mg/kg). Response was assessed as total number GFP+ cells in the femur as determined by flow cytometry of defined volumes (n=5 per group, SEM, * = $p<0.05$).

Supplemental Figure S4. Effects of CTX upon PGE2 expression, the unfolded protein response and senescence in treated leukemia (related to Figure 4). (A) A bar graph showing the level of PGE2 in the bone marrow of leukemia-bearing mice, before and after CTX treatment (n=5 per group, SEM, * = $p<0.05$). **(B)** PCR products resolved on an agarose gel showing XBP-1 splice products before and after CTX treatment. The presence of splice products is characteristic of the unfolded protein

response. **(C)** Time course of morphological changes in leukemia cell-infiltrated tissues after cyclophosphamide therapy. Horizontal columns contain representative samples on the indicated day before or post treatment. Vertical columns show spleen derived H&E stained samples, bone marrow derived H&E stained samples and bone marrow derived samples stained for beta-Galactosidase activity. Counterstaining was performed using nuclear fast red.

Supplemental Figure S5. Analysis of hMB ADCC in the presence of low levels of VEGF and the examination of patient-derived B-ALL for surface expression of CD20 (related to Figure 6). (A) A graph showing the effect of the reduced levels of recombinant VEGF on alemtuzumab-mediated ADCC. The percentage of antibody-mediated phagocytosis in macrophage ADCC was calculated from absolute counts of alemtuzumab treated versus untreated leukemia cells in the macrophage/leukemia cell co-culture (* = $p<0.05$ and *** = $p<0.001$). **(B)** Flow cytometry assessment of the patient-derived B-ALL examined in Figure 6. $CD45^+/CD19^+$ cells were examined for expression of CD20. An isotype control is also shown.

Supplemental Figure S6. Levels of serum TNFα following CTX-containing polychemotherapy (related to Figure 7). A bar graph showing the level of TNFα in bone marrow sera from healthy individuals or B-ALL patients at the indicated times following treatment (* = $p<0.05$).

Supplemental Table Legends

Supplemental Table S1. Oligos used in this study (related to Figure 2). The name, gene target and sequence of all oligos used to make shRNAs for the targeted screen shown in Figure 2 (see the "*In vivo* RNAi-Screening approach" for a description of the approach used to generate shRNAs from these oligos). Additionally, sequencing reads for each shRNA, before and after alemtuzumab treatment, are shown.

Supplemental Table S2. Cytokine Array Data (related to Figure 4). Relative quantitation of all cytokine data, before and after CTX or gamma-irradiation, is shown. Average and mean data are also shown.

Supplemental Table S3. Human Leukemia Descriptions (related to Figure 7). The patient age, leukemia sub-type, karyotype description and Bcr-Abl status of all patient leukemias examined in this study are shown.

Supplemental Experimental Procedures:

Generation of the preB-ALL (hMB) model

We used NOD-SCID-IL2Rg$^{-/-}$ (NSG) mice (Jackson Laboratory) according to protocols approved by the MIT Institutional Animal Care and Use Committee. Human CD133^{+} cells were isolated from cord blood (NDRI) using a combination of Phycoerythrin (PE)-conjugated antibody to human CD133 (Miltenyi) and the EasySep PE Selection Kit (Stem Cell Technologies), according to the manufacturers' protocols. CD133^{+} cells were then cultured *in vitro* in defined media supplemented with several growth factors, as previously described(Zhang et al., 2008). Expanded CD133^{+} cells were re-isolated from the culture using Allophycocyanin (APC)-conjugated anti-human CD133 antibody (Miltenyi) and the EasySep APC Selection Kit (Stem Cell Technologies). Concentrated control or MYC-BCL2-containing lentivirus was added to the cells (MOI = 10-20), as was polybrene (2 µg/ml). The mixture of cells and lentivirus was then plated in 96-well U-bottom plates (Corning) at 1-5×10^{4} cells/100µl/well and centrifuged at 1000×g for 2 hours at 25°C and subsequently cultured at 37°C for an additional 24-48 hours. Adult NSG mice 8-12 weeks of age were irradiated with 2.7 Gy from a ^{137}Cesium source (Gammacell 40, Atomic Energy of Canada), as described previously(Giassi et al., 2008). After 1-3 hours of being irradiated, mice were injected via lateral tail vein injection with 2.5-5×10^{5} CD133^{+} cells that had been exposed to lentivirus. Disease progression in mice was monitored by determining the number of GFP^{+} cells present in 20µl of peripheral blood collected from the lateral tail vein in EDTA. Blood samples were run on an BD Accurri flow cytometer immediately after red blood cell lysis with hypotonic

lysis buffer using a defined 1:30 dilution. Absolute counts of leukemic GFP+ cells in the peripheral blood were calculated accordingly.

Secondary transplant of humanized mouse model

hMB cells were isolated from spleens of late stage primary hMB leukemia mice. Spleens were mechanically dissociated and tissue homogenate filtered with a 70 µm mesh, red blood cells lysed in hypotonic buffer and cells resuspended in PBS. 10^6 hMB cells were immediately transplanted into healthy 6 week old NSG mice and monitored as described above. Upon occurrence of GFP+ leukemia cells in the peripheral blood within a range of 16-24 days treatment was initialized. Peripheral blood leukemia cell burden was assessed in all mice of respective treatment cohort. Mice were stratified to matched treatment cohorts based on peripheral blood leukemia cell count as a proxy for overall tumor burden.

Patient samples and Xenograft models

Patient samples were obtained after informed consent at the University Hospital of Cologne. Peripheral blood was withdrawn prior to treatment initialization and isolated and sorted by Ficoll density centrifugation as previously described. (Pallasch et al., 2009). 10^6 cells were injected to sub-lethally irradiated (2.5 Gy) NRG mice (Pearson et al., 2008). Disease onset was determined by clinical observation and assessment of human $CD45^+/CD19^+$ cells in the peripheral blood.

For analysis of bone marrow macrophage infiltration following chemotherapy, diagnostic flow cytometry assessment of bone marrow aspirates taken from patients at diagnosis and undergoing cyclophosphamide-containing polychemotherapy (GMALL Induction I) at d11 post treatment start. Immunostaining for CD68 was performed on bone marrow smears from 5 ALL prior to therapy and at d11 post therapy onset (lower panel).

Therapeutic regimens

Clinical-grade alemtuzumab (Genzyme) was obtained at a concentration of 30 mg/ml in sterile PBS, and stored at 4°C until needed. To avoid complications from acute tumor lysis syndrome post intravenous injections alemtuzumab was injected at 5 m/kg i.p. at day 1 of treatment followed by an intravenous injection of 5 mg/kg at day 2. Rituximab was obtained from Roche and applied 10 mg/ml. These compounds were then administered via tail vein injection at 5 µl/g mouse body weight. $F(ab)_2$-fragments were generated using pepsin-digest, fluorescently labeled AlexaFluor750-Alemtuzmab was conjugated using the SAIVI Rapid Antibody labeling kit (Invitrogen, Carlsbad CA). Concentration $F(ab)_2$-fragments was determined by competitive binding assay compared to native alemtuzumab by determining AlexaFluor750-Alemtuzmab binding to cells after preincubation in a wide dose-range of $F(ab)_2$-fragmen and full-length alemtuzumab. An equivalent dosage of $F(ab)_2$-fragments was calculated and applied *in vivo* on repeating injection at d2. To avoid complications from acute tumor lysis syndrome post intravenous injections alemtuzumab was injected at 5 m/kg i.p. at day 1 of treatment followed by an intravenous injection of 5 mg/kg at day 2.

In experiments analyzing the timeline of dosing (Figure 4E) a single intraperitoneal injection of 10 mg/kg was applied at the indicated day only.

Chemotherapeutics and radiation therapy

Cyclophosphamide and dexamethasone were obtained from Calbiochem; doxorubicin was obtained from Tocris Bioscience, and fludarabine was obtained from Bayer Schering. Immediately prior to use, chemotherapeutics were weighed and dissolved at follows: cyclophosphamide (10 mg/ml in PBS), fludarabine (30 mg/kg), dexamethasone (0.1 mg/ml in PBS), doxorubicin (0.5 mg/ml in 0.9% NaCl). Chemotherapeutics were then administered via lateral tail vein injection at 10µl/g mouse body weight. 100 ng GM-CSF (Peprotech, Rocky Hill, NJ) was injected subcutaneously twice daily for 6 consecutive days after treatment initialization. Therapeutic irradiation was carried out as 5 Gy total body irradiation.

Generation of macrophages Macrophage mediated antibody dependent cellular cytotoxicity (ADCC) assay. Peritoneal macrophages were generated using 1 ml of thioglycollate broth injected intraperitoneally to healthy mice and macrophages harvested at day4 post injection by intraperitoneal lavage. Bone marrow derived macrophages were generated from bone marrow of healthy mice by co-culture with L929 cell conditioned media containing M-CSF. Macrophages were cultivated in 96-well plates at 10^5 cells per well. For Determination of ADCC absolute cell counts of target cells were analyzed using a BD Accurri flow cytometer, the percentage of specific killing was assessed by quotient of cell counts in antibody containing well vs. untreated well.

Human monocytes were isolated from healthy donor buffy coats (Research Blood Components, Boston) using the RosetteSep human monocyte enrichment cocktail (StemCell Technologies, Vancouver) by untouched depletion in a Ficoll density gradient centrifugation. Human macrophages were differentiated *in vitro* by adherent growth in the presence of 100 ng/ml M-CSF (Peprotech, Rocky Hill).

In vivo depletion of macrophages

Macrophages were depleted *in vivo* via intravenous injections of clodronate liposomes, as previously described (van Rooijen and van Kesteren-Hendrikx, 2003). Clodronate was incorporated into liposomes (0.69 M) (van Rooijen and van Kesteren-Hendrikx, 2003). Clodronate liposomes were stored at 4°C and were warmed to room temperature immediately prior to tail vein injection into recipient mice. Each mouse received 100 µl of the clodronate liposome suspension. 48-72 hours later, splenic macrophage depletion was verified by flow cytometry analysis of splenocytes from recipient mice; macrophages were defined as $CD11b^+$ $CD11c^-$ $Gr\text{-}1^-$ cells, while granulocytes were defined as $CD11b^+$ $Gr\text{-}1^+$ cells.

In vivo RNAi-Screening approach

An 88 shRNA containing library was generated based on prediction by using siRNA Scales (Matveeva et al., 2007) and RNAi central (http://katahdin.cshl.edu). Oligonucleotides were synthesized individually and batch amplified using primers XhoI-for and EcoRI-rev and cloned into our previously published MLS retroviral vector carrying mCHERRY. Amphotropic retrovirus was generated using amphotropic phoenix

cell lines and used for infection of *ex vivo* isolated primary hMB cells. Cells were purified based on mCHERRY-reporter construct and expanded in vitro. 10^6 cells were injected into recipient mice and treatment with alemtuzumab was initialized at d21 post transplant as described above.

Leukemia cells were isolated from spleens at relapse and high-throughput sequencing for representation of shRNA-pools was carried out after PCR-based amplification of specific sequences from genomic DNA. Reads were assigned to specific shRNA sequences and distribution in untreated vs. treated compared for over-representation and depletion of shRNAs. Significant hits were hypothesized to meet the following criteria:

1. A fold change < 0.5 or > 5 respectively
2. At leads 100 total reads in either untreated or alemtuzumab treated groups
3. A p-value of < 0.05 determined by Mann-Whitney-U-Test
4. CV < 1.5

Significant hits were used in sorted single shRNA-infected cells for validation *in vitro* as in *in vivo* (Meacham et al., 2009).

Microscopy

Live cell imaging of antibody directed leukemia cell phagocytosis was performed using a 20x magnification on a Delta Vision or Nikon Confocal microscope. Macrophage counts in bone marrow and spleen tissue was assessed on an Olympus FV1000 multiphoton

laser scanning confocal microscope applying an inverted 20x objective at 810 nM excitation wavelength.

Histology

Tissues were fixed in formaldehyde and embedded in paraffin. Sections were stained with Giemsa, hematoxylin/eosin or nuclear fast read respectively. For detection of senescence bone marrow pieces were extracted from tibia heads, and stained in total using senescence beta-Gal staining kit (Cell Signaling) at 37° over night. Tissue was subsequently embedded in paraffin and counter-stained with nuclear-fast-red.

Cell Sorting

GFP+ labeled hMB cells were sorted using BD FACS ARIA and MoFLo (Coulter). hMB cells for *in vitro* assays and generation of conditioned media were separated by human $CD19^+$ positive selection using magnetic beads (Stemcell Technologies).

Cytokine Profiling

Tibia of untreated, irradiated or cyclophosphamide treated mice were dissected and flushed with 200 µl of PBS. Samples were lysed with 0.1 % NP-40 and subjected to a 65 human cytokine multiplex assay performed by the manufacturer at Eve-technologies (Calgary, Canada).

XBP1 splicing assay

Total mRNA was isolated from cells using Qiashredder and RNeasy kits from Qiagen. cDNA was made from 100ng or 1µg of RNA using random hexamers and M-MLV reverse transcriptase from Invitrogen. The XBP1 PCR was preformed as previously described (Calfon et al., 2002).

Statistics

Expected additive drug effects of alemtuzumab and cyclophosphamide (P_{ac}) were calculated as $P_{ac} = P_a + P_c – (P_a \times P_c)$ (P_a = alemtuzumab-mediated toxicity; P_c = cyclophosphamide-mediated toxicity) (Verrier et al., 2001).

Supplemental References

Calfon, M., Zeng, H., Urano, F., Till, J.H., Hubbard, S.R., Harding, H.P., Clark, S.G., and Ron, D. (2002). IRE1 couples endoplasmic reticulum load to secretory capacity by processing the XBP-1 mRNA. Nature *415*, 92-96.

Giassi, L.J., Pearson, T., Shultz, L.D., Laning, J., Biber, K., Kraus, M., Woda, B.A., Schmidt, M.R., Woodland, R.T., Rossini, A.A.*, et al.* (2008). Expanded CD34+ human umbilical cord blood cells generate multiple lymphohematopoietic lineages in NOD-scid IL2rgamma(null) mice. Exp Biol Med (Maywood) *233*, 997-1012.

Jackson, S.H., Gallin, J.I., and Holland, S.M. (1995). The p47phox mouse knock-out model of chronic granulomatous disease. The Journal of experimental medicine *182*, 751-758.

Matveeva, O., Nechipurenko, Y., Rossi, L., Moore, B., Saetrom, P., Ogurtsov, A.Y., Atkins, J.F., and Shabalina, S.A. (2007). Comparison of approaches for rational siRNA design leading to a new efficient and transparent method. Nucleic acids research *35*, e63.

Meacham, C.E., Ho, E.E., Dubrovsky, E., Gertler, F.B., and Hemann, M.T. (2009). In vivo RNAi screening identifies regulators of actin dynamics as key determinants of lymphoma progression. Nature genetics *41*, 1133-1137.

Pallasch, C.P., Patz, M., Park, Y.J., Hagist, S., Eggle, D., Claus, R., Debey-Pascher, S., Schulz, A., Frenzel, L.P., Claasen, J.*, et al.* (2009). miRNA deregulation by epigenetic silencing disrupts suppression of the oncogene PLAG1 in chronic lymphocytic leukemia. Blood *114*, 3255-3264.

Pearson, T., Shultz, L.D., Miller, D., King, M., Laning, J., Fodor, W., Cuthbert, A., Burzenski, L., Gott, B., Lyons, B.*, et al.* (2008). Non-obese diabetic-recombination activating gene-1 (NOD-Rag1 null) interleukin (IL)-2 receptor common gamma chain (IL2r gamma null) null mice: a radioresistant model for human lymphohaematopoietic engraftment. Clinical and experimental immunology *154*, 270-284.

van Rooijen, N., and van Kesteren-Hendrikx, E. (2003). "In vivo" depletion of macrophages by liposome-mediated "suicide". Methods Enzymol *373*, 3-16.
Verrier, F., Nadas, A., Gorny, M.K., and Zolla-Pazner, S. (2001). Additive effects characterize the interaction of antibodies involved in neutralization of the primary dualtropic human immunodeficiency virus type 1 isolate 89.6. J Virol *75*, 9177-9186.

Zhang, C.C., Kaba, M., Iizuka, S., Huynh, H., and Lodish, H.F. (2008). Angiopoietin-like 5 and IGFBP2 stimulate ex vivo expansion of human cord blood hematopoietic stem cells as assayed by NOD/SCID transplantation. Blood *111*, 3415-3423.

Supplemental Figure S1

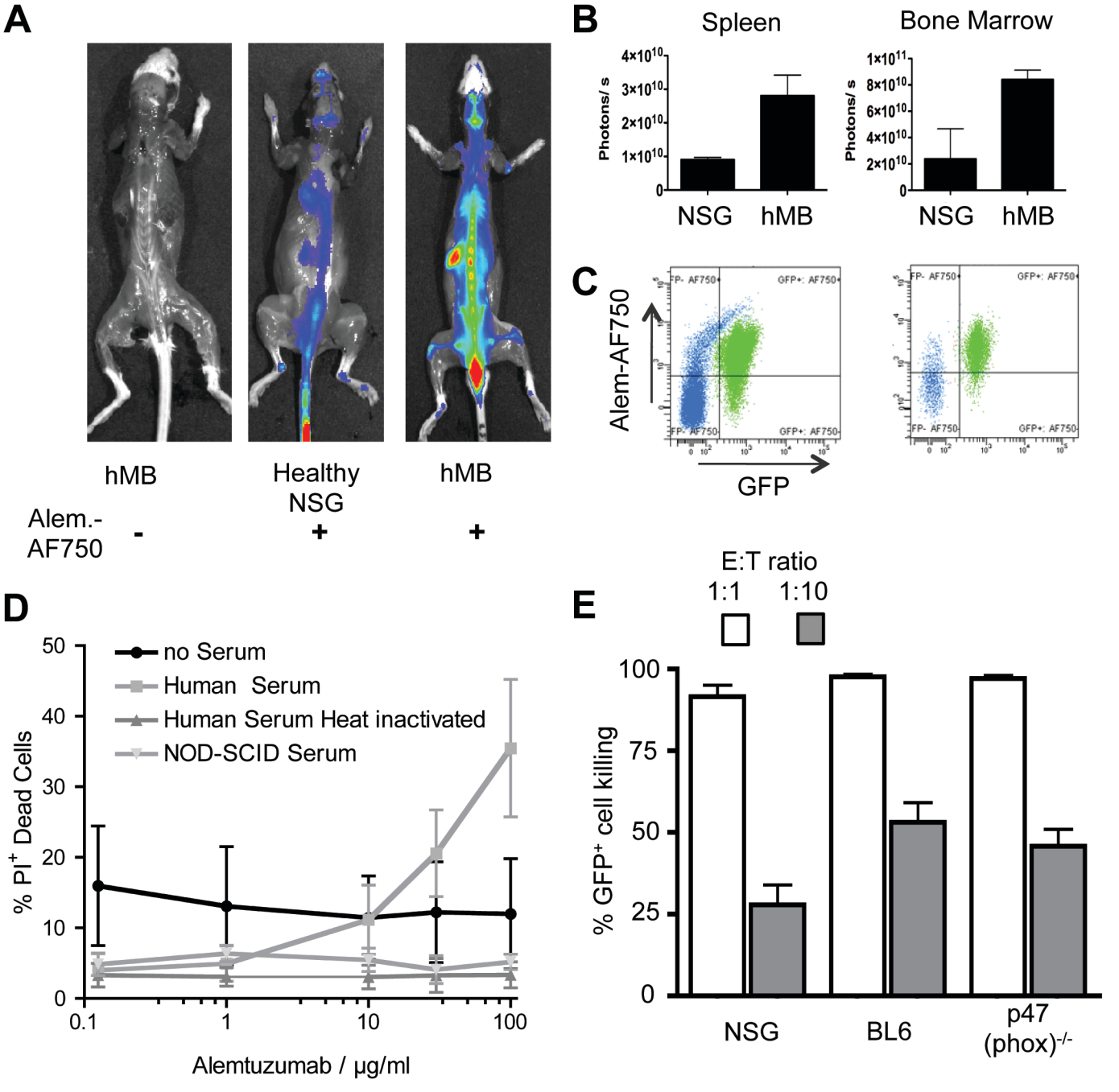

Supplemental Figure S2

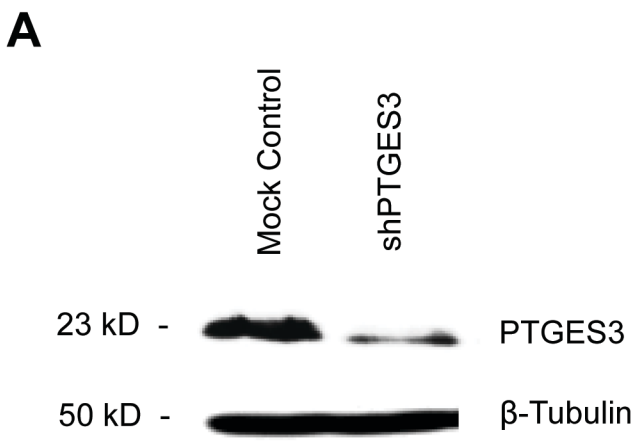

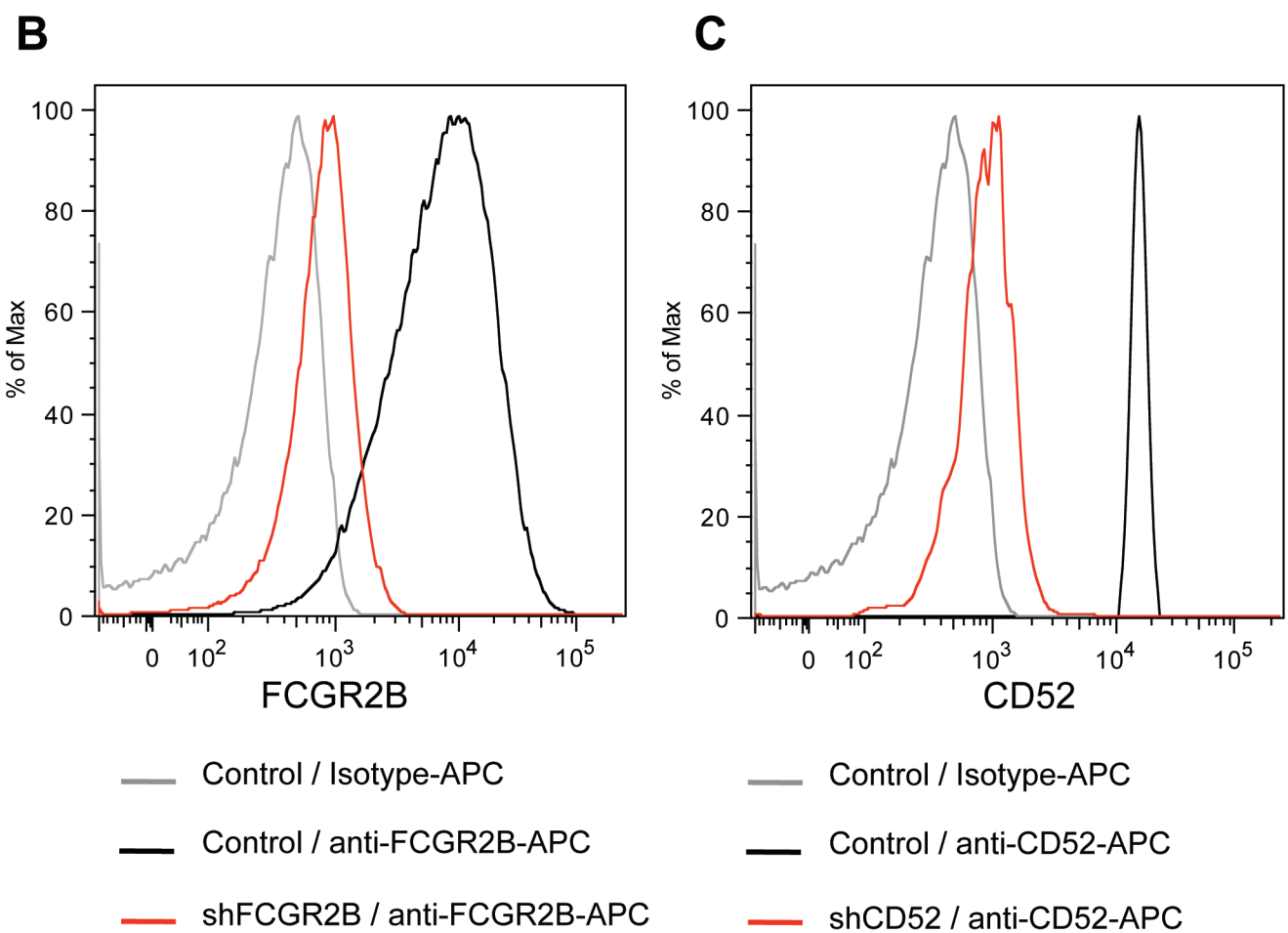

Supplemental Figure S3

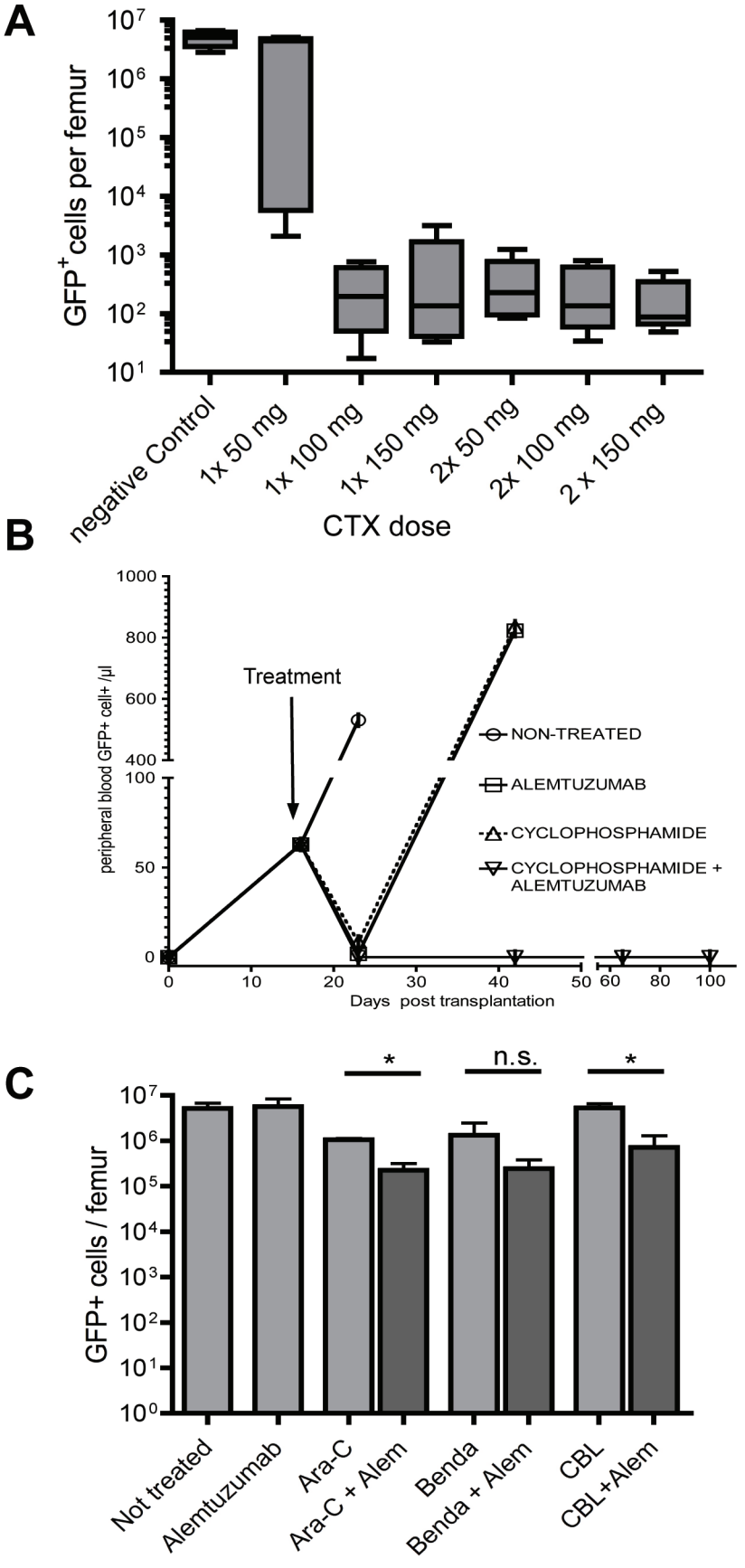

Supplemental Figure S4